AD-A044 178 ARMY INST OF DENTAL RESEARCH WASHINGTON D C F/G 6/5
EFFECTS OF CO2 LASER RADIATION ON ORAL SOFT TISSUES: AN INITIAL--ETC(U)
SEP 77 J C ADRIAN

UNCLASSIFIED NL

| OF |
AD
A044 178

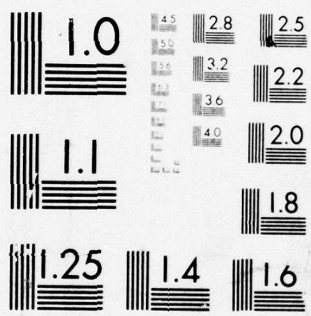

MICROCOPY RESOLUTION TEST CHART
NATIONAL BUREAU OF STANDARDS-1963-A

Unclassified
SECURITY CLASSIFICATION OF THIS PAGE (When Data Entered)

REPORT DOCUMENTATION PAGE

READ INSTRUCTIONS BEFORE COMPLETING FORM

1. REPORT NUMBER	2. GOVT ACCESSION NO.
3. RECIPIENT'S CATALOG NUMBER	
4. TITLE (and Subtitle) EFFECTS OF CO_2 LASER RADIATION ON ORAL SOFT TISSUES: AN INITIAL REPORT.	5. TYPE OF REPORT & PERIOD COVERED Manuscript for publication Jun 77-Sep 77
	6. PERFORMING ORG. REPORT NUMBER
7. AUTHOR(s) COL James C. Adrian	8. CONTRACT OR GRANT NUMBER(s) Rept. for Jun-Sep 77
9. PERFORMING ORGANIZATION NAME AND ADDRESS U.S. Army Institute of Dental Research, Walter Reed Army Medical Center, Washington, D.C. 20012	10. PROGRAM ELEMENT, PROJECT, TASK AREA & WORK UNIT NUMBERS 611101.91.7.35941 00-360
11. CONTROLLING OFFICE NAME AND ADDRESS U.S. Army Med. Research & Development Cmd, HQDA (SGRD-RP), Washington, D.C. 20314	12. REPORT DATE 12 Sep 77
	13. NUMBER OF PAGES ~~17~~ 12 35p.
14. MONITORING AGENCY NAME & ADDRESS (if different from Controlling Office)	15. SECURITY CLASS. (of this report) Unclassified
	15a. DECLASSIFICATION/DOWNGRADING SCHEDULE

16. DISTRIBUTION STATEMENT (of this Report)

This document has been approved for public release and sale; its distribution is unlimited.

17. DISTRIBUTION STATEMENT (of the abstract entered in Block 20, if different from Report)

18. SUPPLEMENTARY NOTES

19. KEY WORDS (Continue on reverse side if necessary and identify by block number)

1. Laser
2. CO_2 Laser
3. Non-ionizing Radiation
4. Oral Soft Tissue
5. Laser effects on Soft Tissue
6. Homogenized Collagen
7. Basement Membrane
8. Vessel coagulation

20. ABSTRACT (Continue on reverse side if necessary and identify by block number)

Three different oral mucosal sites were exposed to the CO_2 surgical laser. Although nearly every laser exposure caused the loss of the epithelium and penetration of the lamina propria up to 0.5 mm., no bleeding occurred. Histologic changes included shredding of keratin, vacuole formation and basal cell degeneration in the epithelium. Glassy homogenization of collagen and vascular occlusion characterize the alterations in the connective tissue. These changes were consistent for each of the three tissues examined. Within the limits of the experimental procedure, it appears that the laser vaporizes an additional 0.1 mm.

DD FORM 1 JAN 73 1473 EDITION OF 1 NOV 65 IS OBSOLETE

Unclassified
SECURITY CLASSIFICATION OF THIS PAGE (When Data Entered)

of tissue for each 5 watt increase in power when the time of exposure remains constant.

EFFECTS OF CO_2 LASER RADIATION ON ORAL SOFT TISSUES: AN INITIAL REPORT

James C. Adrian, BS, DDS, MS*

Division of Pathology
U.S. Army Institute of Dental Research
Walter Reed Army Medical Center
Washington, D.C. 20012

* Chief, Division of Pathology and Surgery

The CO_2 laser as a surgical instrument has been used for microsurgery in the aerodigestive tract in both experimental animals and humans.[1,2,3,4] In contrast to the ruby and neodymium lasers, the CO_2 laser is almost completely absorbed by biologic tissues. CO_2 laser tissue destruction is entirely a thermal process and has an extraordinary hemostatic effect.[2] In one study[2] segmental resections of the canine tongue and soft palate were carried out with no bleeding unless a vessel greater than 0.5 mm was sectioned; and even these vessels could be secondarily coagulated by the laser. In a recent study,[5] the ventral surface of the tongue of a dog was exposed to CO_2 laser impacts. There was no bleeding and short term follow up (3 weeks) indicated that healing was progressing normally.

The purpose of this investigation is the following:

1. To study the CO_2 laser and to establish baseline data of the response of various oral tissues to the laser.

2. To evaluate the feasability of the use of the CO_2 laser in incision, excision and wound debridement.

Method and Material:

A CO_2 laser system* and a rhesus monkey were used in this initial study. The animal was placed under IV anesthesia using 8 mg. of pentobarbital and 2.5 mg of Sernylan** per Kg. of body weight. The tissue surface to be exposed was held perpendicular to the incident laser beam and the laser

* Coherent Medical, Palo Alto, Ca.
** BIO-CEUTIC Laboratories Inc. St Joseph, Mo.

focused to a 2 mm spot using a 400 mm focal length lens.

Each tissue surface was exposed using the following schedule:

	5 Watts	10 Watts	20 Watts
Ventral Surface of Tongue	4 Impacts	4 Impacts	4 Impacts
Labial Mucosa	4 Impacts	4 Impacts	4 Impacts
Gingiva	4 Impacts	4 Impacts	4 Impacts

All exposures were 0.5 sec. in length.

The animal was sacrificed immediately post exposure. The tissues were harvested and fixed in 10% buffered formalin. The following staining procedures were done on each specimen: 1. Hematoxylin and Eosin (H&E) 2. Massons Trichrome 3. Periodic Acid Schiff (PAS).

The tissues were evaluated using light microscopy for effects on the epithelium, collagen, and the basement membrane. The diameter and depth of the impacted site was measured with a filar micrometer attachment on the microscope. A determination of the size and extent of damage to the remaining tissues was made using light microscopic changes (i.e - vacuolation in cells, intracellular edema, nuclear changes, coagulation of tissue proteins and carbonization).

Results:

Clinical Impressions -

At the time of impact, a small puff of smoke and/or steam was seen. This was easily controlled by a suction device. In addition, the more loosely bound tissues (Ventral surface of the tongue and labial mucosa) demonstrated a slight shrinkage or an apparent drawing toward the center of the impact area. This did not seem to occur as readily in the gingiva. There was never any evidence of bleeding during the entire experimental period.

Immediately post impact, the base of the crater appeared rather flat. The margins of the crater were slightly raised and were light brown due to tissue charring. There was also a small amount of debris on the crater floor. The margin of the crater was surrounded by a halo of blanched tissue approximately 1 mm. in width.

Histologic Findings -

The mean width and depth of the tissue void (crater) caused by the CO_2 laser are given in table 1. In table 2, the mean values represent the extent of the microscopic alteration of the tissue remaining at the lateral and deep margins of the crater.

The tissue changes are characterized by the following:

1. Gingiva - 5 Watts

   Epithelium - Vacuolization of the superficial layers, detachment and laminated shredding of keratin, basal cell degeneration and separation from the lamina propria are the chief features. In some foci the epithelium is very thin (1-2 cell layers) but appears intact in all sections (Fig. 1,2,3).

   Connective Tissue - While there is no change in the superficial lamina propria evident in the H&E sections, the Masson Stain reveals a very thin layer (0.005 mm) of altered connective tissue at the tips of the dermal papillae. A PAS stain (Fig. 4) reveals the presence of the basement membrane which appears to be more dense or darker staining in the area of laser impact.

2. Gingiva - 10 Watts

   Epithelium - the epithelium is completely lost in the central part of the crater. At the crater edges the changes seen are vacuole formation, keratin separation, prickle cell shrinkage and basal cell degeneration characterized by pyknotic nuclei and marked vacuolization of the cytoplasm. These changes become less intense as one proceeds to the periphery of the impact site. The epithelial remnants remaining at the periphery of the crater appear to tip inward toward the void (Fig. 5).

Connective Tissue - Several small occluded vascular channels are seen immediately below the surface. The connective tissue papillae are grossly intact. However, both the Masson and H&E stains reveal altered collagen characterized by a homogenized, glassy appearance (Fig. 6). The basement membrane with intensified PAS staining is for the most part, present throughout the sections.

3. Gingiva - 20 Watts

Epithelium - There is complete loss of the epithelium in the crater area. The changes at the margin are similar to those noted above.

Connective Tissue - The base appears relatively flat with complete loss of the connective tissue papillae (Fig. 7). The basement membrane is also lost in this area but remains intact beneath the epithelium at the periphery of the crater. The intensified staining characteristic of the basement membrane persists in the PAS sections. The glassy homogenization of the collagen fibers and occluded vessels are also seen.

4. Tongue - 5 Watts

Epithelium - There is complete loss of the epithelium in the center of the crater. At the periphery of the crater the epithelial cell walls are damaged so that the remaining epithelium has the appearance of a confluent mass of coagulated material with elongated, thin pyknotic nuclei. There is no orthokeratin layer present in this tissue.

Connective Tissue - The basement membrane appears intact and stains more intensely with PAS in the area of laser exposure than in unexposed area. There is loss of the small, distinct collagen fibers and replacement with homogenous confluent bundles. The connective tissue papillae are grossly intact (Fig. 8).

5. Tongue - 10 Watts

Epithelium - There is complete loss of the epithelium across the area of impact. The parakeratin material at the periphery is separating and lifting off the prickle cell layer. The basal cells of the rete ridges immediately adjacent to the void are shrunken, vacuolated and have lost their attachment to the basement membrane.

Connective Tissue - The connective tissue papillae of the lamina propria are present. The basement membrance covering them for the most part remains intact. There is homogeneous coagulation of the collagen bundles.

6. Tongue - 20 Watts

Epithelium - At the periphery, the epithelium is vacuolated, some shedding of the parakeratin is present and the basal cells demonstrate small cytoplasmic vacuoles and pyknotic nuclei. There is separation of the epithelium from the underlying connective tissue at the crater margin. No epithelium remains in the central crater area.

Connective Tissue - The crater base is irregular with the center appearing convex when viewed from the surface (Fig. 9). The peripheral areas of the crater base immediately beneath the edge of the remaining epithelium seem to plunge deeper into the connective tissue than the crater center. This accounts for the microscopic convex appearance of the floor of the crater. The basement membrane is lost in the center but again appears more prominent with the PAS stain beneath the remaining epithelial cover. Several muscle fibers are involved at the base of the crater and large steam vacuoles may be seen within the fibers (Fig. 10). The remaining muscle substance surrounding the vacuoles appears glossy and homogenous. Numerous occluded vessels are present along with a rather large diameter nerve fiber upon which the principal effect seem to be loss of the myelin sheath surrounding the individual fibers (Fig. 11,12).

7. Labial Mucosa - 5 Watts

These specimens were lost in tissue processing.

8. Labial Mucosa - 10 Watts

Epithelium - All epithelium is lost in the area of the crater. At the periphery, the basal layer of the remaining epithelium is the most severely affected portion exhibiting the changes previously described.

Connective Tissue - The basement membrane remains essentially intact throughout the impact area. The dermal papillae, although not normally as frequent or as pronounced as in the gingiva, remain microscopically visible. Homogenized collagen with occasional occluded vessels are noted (Fig. 13, 14).

9. Labial Mucosa - 20 Watts

Epithelium - No epithelium remains in the central portion of the crater. At the periphery, steam vacuoles, basal cell changes, loss of connective tissue attachment and occasional carbonization are present.

Connective Tissue - Homogenization of collagen, small vessel occlusion and obliteration of the dermal papillae characterize the changes noted in the specimen. In addition, no basement membrane is seen in the crater center.

Carbonization of varying amounts was noted in all sections of every power density.

Discussion:

It may be seen from Table 1 that the depth of the void caused by the laser beam is quite consistant between the various tissue sites at the same power output. As the power output increases, of course, the depth of pentration is greater. This reflects the very similiar water content of the soft tissue and increased power density at the site. There is much greater variation (Table 1) in the width of the crater than in the depth. Table II also shows a much larger variation in the lateral tissue changes as opposed to the deep tissue changes noted in the histopathologic specimens. The author attributes this variation to a combination of factors including: 1. Slight lateral movement of the activated laser by the operator. 2. Slight movement of the animal. 3. Minor deviation from the focal plane of the laser beam which will produce a slightly larger area of impact.

These factors may account for variation in lateral tissue changes but they would not have an appreciable effect on the deep tissue changes since the slight lateral movements would not cause the beam to be removed from the deep area of tissue contact. This is substantiated by the low standard deviation of the depth and base effects seen in tables 1 and 2 respectively.

The histopathologic changes seen in our material are not appreciably different from those of other investigators.[2,5,6] However, we have found only one previous report in the literature of the effects of the CO_2 laser on the basement membrane. Mihashi and others[5] note in their transmission electron micrographs that the basement membrane is missing. In our study the basement membrane was consistently present at 5 watts, intermittent at 10 watts and missing at 20 watts as revealed by the PAS stain.

The epithelial portion of the mucous membrane was either intact, albeit thin, or intermittently absent in the 5 watt exposures. The connective tissue elements at 5 watts showed a very slight effect on the collagen.

At 10 watts, the epithelium is completely missing from the crater base but the dermal papillae are frequently preserved. There is more extensive alteration in the connective tissue. Glassy homogenization of collagen, occluded vessels and steam vacuoles are seen.

No epithelium is present in the base of the crater at 20 watts. The dermal papillae are gone and steam vacuoles, homogenized collagen and occluded vessels are seen in the crater base.

The base of the crater occasionally presents a convex appearance when viewed from the surface. It appears that the effect of the laser beam in these instances is more intense at the intersection of the lateral and deep walls of the crater than in the center. These effects would seem to be contrary to the expected effect of the wave front, ie. deeper in the center of the crater rather than at the edges. This unusual appearance of the base of the crater only occured at 20 watts in the labial mucosa and the ventral surface of the tongue. It also has been previously reported in the literature in the ventral surface of the tongue.[5] It is our belief that this is a result of the shrinkage of the tissue due to the heat coagulation of the collagen. As the collagen is coagulated, it shrinks more intensely in the center and draws the more loosely bound surrounding tissues toward the center. This causes the edges of the crater base to appear to extend more deeply into the underlying tissues than the center. Hence, the seeming convexity of the crater base. In the gingiva where the lamina propria is more tightly bound to the supporting bone, this phenomenon did not occur. Compare figures 7 and 9.

It has been noted that during all of the surgical procedures, there was no bleeding. This appears to be related to the shrinkage and coagulation of both the vessels per se and the connective tissue surrounding them.

Carbonization of tissue elements occured in all specimens but we were unable to adequately quantify the material so that any useful information might be obtained from it.

There was no evidence of either inflammation or healing in any of our material due to the immediate sacrifice interval.

An examination of the crater depth in Table 1 suggests that when the time remains constant, each 5 watt increase of the power output causes approximately 0.1 mm of additional tissue to be vaporized.

It is the opinion of the author that the lack of hemorrhage, ease and speed of laser manipulation and predictable tissue effects definitely militate in favor of further investigations in the area of laser excision and wound debridement.

Table I

Width and Depth of the Tissue Crater Caused by CO_2 Laser Radiation*

	5 Watts		10 Watts		20 Watts	
	Width	Depth	Width	Depth	Width	Depth
Gingiva	1.92	0.21	1.59	0.36	1.98	0.54
Ventral Surface of Tongue	1.47	0.18	2.04	0.24	2.49	0.45
Labial Mucosa	**		1.32	0.27	1.95	0.45
Mean Values	1.7	0.20	1.7	0.29	2.14	0.48
Standard Deviation of the Mean	0.225	0.016	0.301	0.051	0.248	0.042

* All measurements are given in millimeters and represent the average of 10 readings.

** Specimens lost in processing.

Table II

Extent of Microscopic Alteration in Marginal Tissue[1]

	5 Watts		10 Watts		20 Watts	
	Lateral (2) Margin	Deep (3) Margin	Lateral Margin	Deep Margin	Lateral Margin	Deep Margin
Gingiva	0.75	0.01	0.84	0.11	1.11	0.18
Ventral Surface of Tongue	0.57	0.03	1.00	0.06	1.05	0.31
Labial Mucosa	(4)		0.50	0.21	0.78	0.23
Mean Values	0.66	0.02	0.78	0.13	0.98	0.24
Standard Deviation of the Mean	0.09	0.01	0.256	0.062	0.144	0.054

1. All measurements are in millimeters and represent the average of 10 readings.
2. All lateral measurements are in epithelium.
3. All deep measurement are in connective tissue.
4. Specimens lost in processing.

Abstract

Three different oral mucosal sites were exposed to the CO_2 surgical laser. Although nearly every laser exposure caused the loss of the epithelium and penetration of the lamina propria up to 0.5 mm., no bleeding occurred. Histologic changes included shredding of keratin, vacuole formation and basal cell degeneration in the epithelium. Glassy homogenization of collagen and vascular occlusion characterize the alterations in the connective tissue. These changes were consistent for each of the three tissues examined. Within the limits of the experimental procedure, it appears that the laser vaporizes an additional 0.1 mm. of tissue for each 5 watt increase in power when the time of exposure remains constant.

BIBLIOGRAPHY

1. Jako, Geza J.: Laser Surgery of the Vocal Cords. An Experimental Study with Carbon Dioxide Lasers on Dogs. The Laryngoscope. Vol. 82, No. 12, pp. 2204-2216, December 1972.

2. Strong, M. Stuart and Jako, Geza J.: Laser Surgery in the Larynx. Early Clinical Experience with Continuous CO_2 Laser. Ann Otol, 81:791-798, 1972.

3. Strong, M. Stuart, et. al.: Laser Surgery in the Aerodigestive Tract. The American Journal of Surgery, 126:529-533, October 1973.

4. Andrews, Albert H. Jr. and Moss, Harold W.: Experiences with the Carbon Dioxide Laser in the Larynx. Annals of Otology, Rhinology and Laryngology, 83:462-470, July-August, 1974.

5. Mhashi, S., et al.: Laser Surgery in Otolaryngology: Interaction of CO_2 Laser and Soft Tissue. Ann. N.Y. Acad. Sc, 267:263-293, 1976.

6. Stellar, S.: The Carbon Dioxide Laser in Experimental and Clinical Surgery for Neoplasms. Panminerva Medica, 17:223-228, 1975.

In conducting the research described in the manuscript, the investigators adhered to the "Guide for the Care and Use of Laboratory Animals", as promulgated by the Committee on the Guide for Laboratory Animal Facilities and Care of the Institute of Laboratory Animal Resources, National Academy of Sciences - National Research Council.

Legends for Illustrations

Fig. 1. Gingiva, 5 watts. Tissue changes characterized by vacuole formation (Fig. 2) and shredding of keratin (Fig. 3) in the superficial epithelium and basal cell degeneration and separation from the lamina propria in deep epithelial layers. (H&E: Magnification X120).

Fig. 2. Gingiva, 5 watts. High power photomicrograph demonstrating vacuole formation in the superficial layers of the epithelium (upper left in photo) and basal cell degeneration and epithelial separation. (H&E; Magnification X300).

Fig. 3. Gingiva, 5 watts. High power photomicrograph demonstrating shredding and vacuolization in the keratin layer and basal cell degeneration and separation from the lamina propria by the epithelium. (H&E; Magnification X300).

Fig. 4. Gingiva, 5 watts. A photomicrograph of a PAS stained specimen which demonstrates the intense staining character of the basement membrane. (PAS; Magnification X300).

Fig. 5. Gingiva, 10 watts. Lower power photomicrograph of the impact site. The left edge of the photograph is in the center of the crater. The epithelium is completely lost in the center of the crater but the connective tissue papillae remain (Fig. 6). The epithelial changes include vacuolization, keratin shredding and epithelial separation. The epithelium near the crater edge appears to "lean" toward the void. (H&E; Magnification X46).

Fig. 6. Gingiva, 10 watts. Photomicrograph of the tissue in the base of the crater. The connective tissue papillae remain while all the epithelial covering is lost. At the surface vacuoles are noted, but beneath the surface, small occluded vessels and homogenized, glassy collagen can be seen extending to a depth of 0.11 mm (See Chart 2). (H&E; Magnification X285).

Fig. 7. Gingiva, 20 watts. The center of the crater is to the left. At the base of the crater note the flat appearance with the loss of the dermal papillae. At the crater edge the papillae remain. The epithelial changes are vacuolization, keratin shreeding and separation from the lamina propria. The depth of the altered connective tissue gradually decreases from the center to the periphery of the impact area. (H&E; Magnification X100).

Fig. 8. Tongue, 5 watts. The epithelial covering is completely lost in the crater center but the connective tissue papillae remain. (H&E; Magnification X100).

Fig. 9. Tongue, 20 watts. A low power photomicrograph demonstrating to convex appearance of the base of the laser crater. (Masson. Magnification X40). (See also Figures 10, 11 & 12).

Fig. 10. Tongue, 20 watts. A high power photomicrograph from the surface of the crater base seen in Fig. 9, demonstrating the steam vacuole formation within the muscle fibers. (Masson. Magnification X640).

Fig. 11. Tongue, 20 watts. A high power photomicrograph of a nerve fiber taken from normal tissue in Fig. 9. Note the dark rings of myelin surrounding the axons and the fibriller character of the collagenous connective tissue supporting the nerve fiber. (Masson. Magnification X640).

Fig. 12. Tongue, 20 watts. A high power photomicrograph of a nerve fiber immediately beneath the surface of the crater base seen in Fig. 9. The surrounding connective tissue has a homogenized, glassy appearance. By comparison with the normal nerve seen in Fig. 11, one should note the lack of staining ability of the myelin sheath and numerous pyknotic nuclei of the supporting Schwann cells. (Masson. Magnification X640).

Fig. 13. Labial Mucosa, 10 watts. A low power photomicrograph providing an overview of the impact area. The gradation of the tissue changes may be seen as one proceeds from the center to either edge. (See Fig. 14). (H&E; Magnification X48).

Fig. 14. Labial Mucosa, 10 watts. A high power photomicrograph of the central area of the crater base demonstrated in Fig. 13 in which may be seen dermal papillae at the surface and shrunken occluded vessels within the homogenous, confluent collagen in the lamina propria. (H&E; Magnification X160).

Fig. 1. Gingiva, 5 watts. Tissue changes characterized by vacuole formation (Fig. 2) and shredding of keratin (Fig. 3) in the superficial epithelium and basal cell degeneration and separation from the lamina propria in deep epithelial layers. (H&E: Magnification X120).

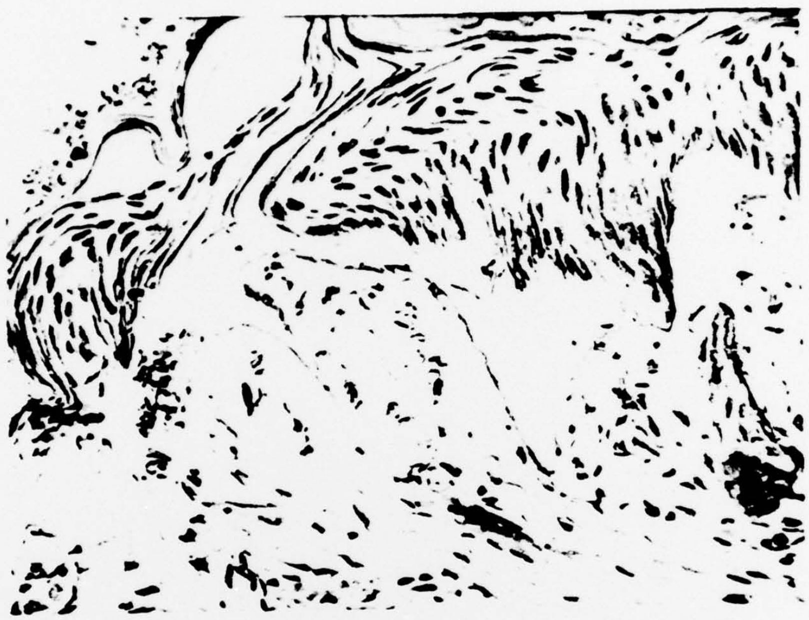

Fig. 2. Gingiva, 5 watts. High power photomicrograph demonstrating vacuole formation in the superficial layers of the epithelium (upper left in photo) and basal cell degeneration and epithelial separation. (H&E; Magnification X300).

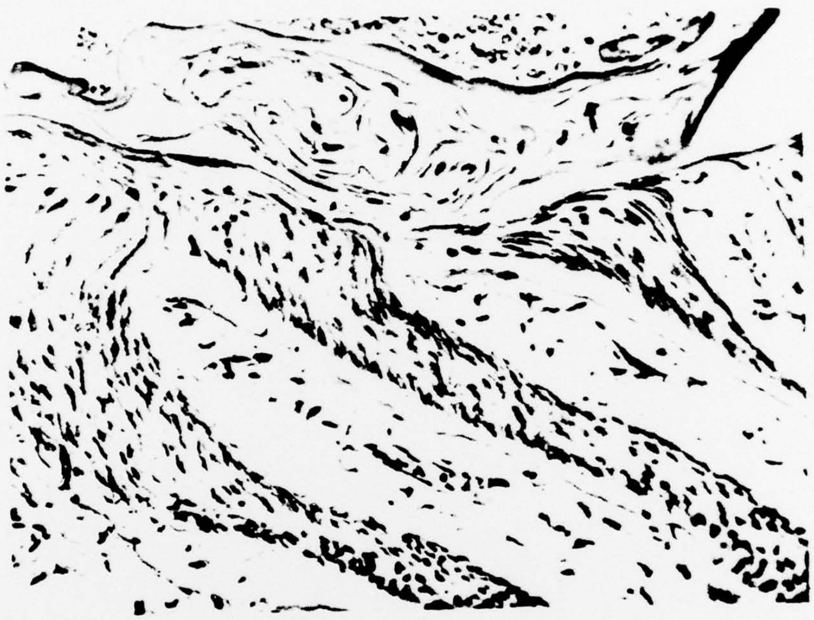

Fig. 3. Gingiva, 5 watts. High power photomicrograph demonstrating shredding and vacuolization in the keratin layer and basal cell degeneration and separation from the lamina propria by the epithelium. (H&E; Magnification X300).

Fig. 4. Gingiva, 5 watts. A photomicrograph of a PAS stained specimen which demonstrates the intense staining character of the basement membrane. (PAS; Magnification X300).

Fig. 5. Gingiva, 10 watts. Lower power photomicrograph of the impact site. The left edge of the photograph is in the center of the crater. The epithelium is completely lost in the center of the crater but the connective tissue papillae remain (Fig. 6). The epithelial changes include vacuolization, keratin shredding and epithelial separation. The epithelium near the crater edge appears to "lean" toward the void. (H&E; Magnification X46).

Fig. 6. Gingiva, 10 watts. Photomicrograph of the tissue in the base of the crater. The connective tissue papillae remain while all the epithelial covering is lost. At the surface vacuoles are noted, but beneath the surface, small occluded vessels and homogenized, glassy collagen can be seen extending to a depth of 0.11 mm (See Chart 2). (H&E; Magnification X285).

Fig. 7. Gingiva, 20 watts. The center of the crater is to the left. At the base of the crater note the flat appearance with the loss of the dermal papillae. At the crater edge the papillae remain. The epithelial changes are vacuolization, keratin shreeding and separation from the lamina propria. The depth of the altered connective tissue gradually decreases from the center to the periphery of the impact area. (H&E; Magnification X100).

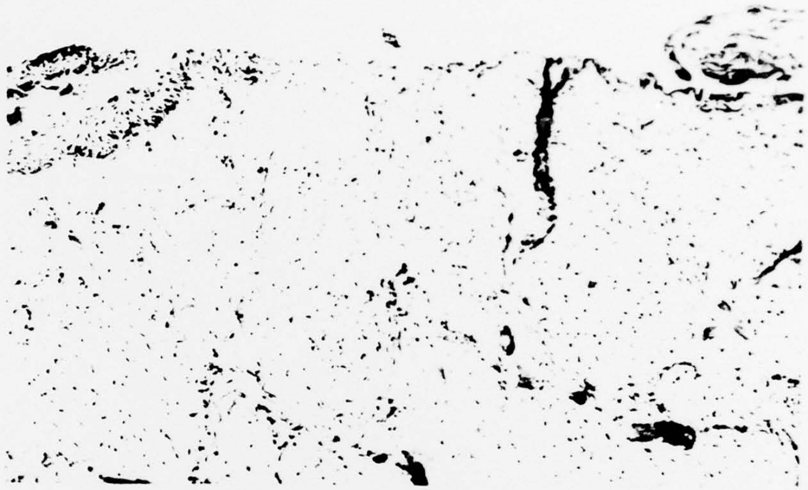

Fig. 8. Tongue, 5 watts. The epithelial covering is completely lost in the crater center but the connective tissue papillae remain. (H&E; Magnification X100).

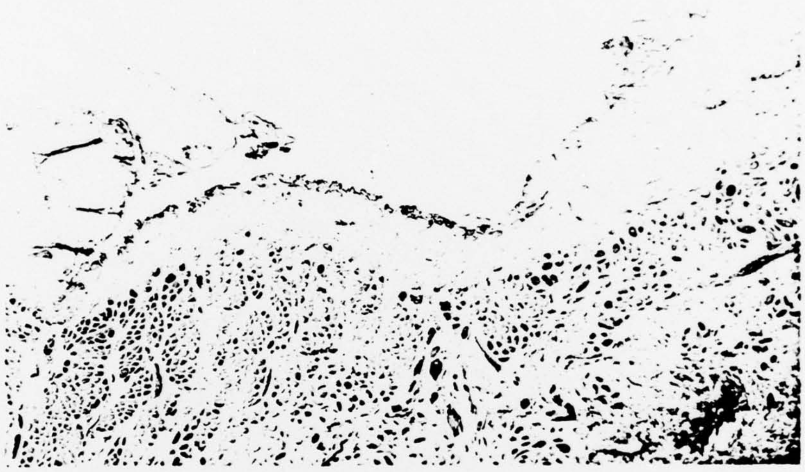

Fig. 9. Tongue, 20 watts. A low power photomicrograph demonstrating to convex appearance of the base of the laser crater. (Masson. Magnification X40). (See also Figures 10, 11 & 12).

Fig. 10. Tongue, 20 watts. A high power photomicrograph from the surface of the crater base seen in Fig. 9, demonstrating the steam vacuole formation within the muscle fibers. (Masson. Magnification X640).

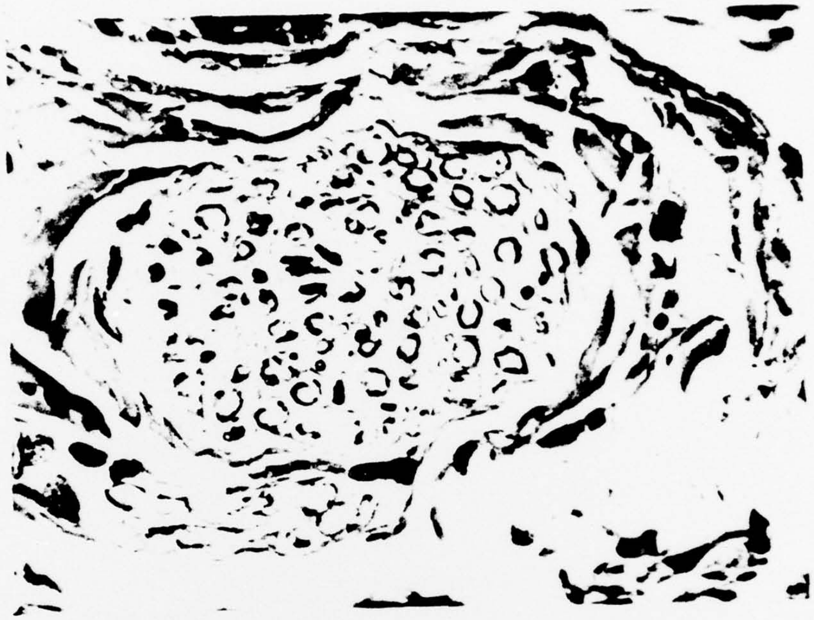

Fig. 11. Tongue, 20 watts. A high power photomicrograph of a nerve fiber taken from normal tissue in Fig. 9. Note the dark rings of myelin surrounding the axons and the fibriller character of the collagenous connective tissue supporting the nerve fiber. (Masson. Magnification X640).

Fig. 12. Tongue, 20 watts. A high power photomicrograph of a nerve fiber immediately beneath the surface of the crater base seen in Fig. 9. The surrounding connective tissue has a homogenized, glassy appearance. By comparison with the normal nerve seen in Fig. 11, one should note the lack of staining ability of the myelin sheath and numerous pyknotic nuclei of the supporting Schwann cells. (Masson. Magnification X640).

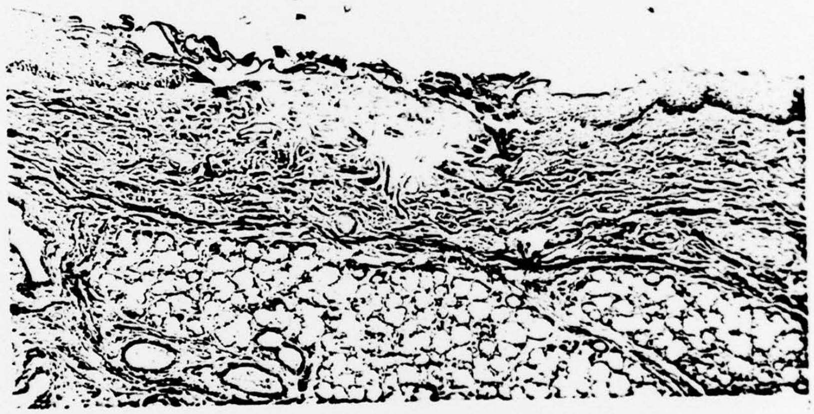

Fig. 13. Labial Mucosa, 10 watts. A low power photomicrograph providing an overview of the impact area. The gradation of the tissue changes may be seen as one proceeds from the center to either edge. (See Fig. 14). (H&E; Magnification X48).

Fig. 14. Labial Mucosa, 10 watts. A high power photomicrograph of the central area of the crater base demonstrated in Fig. 13 in which may be seen dermal papillae at the surface and shrunken occluded vessels within the homogenous, confluent collagen in the lamina propria. (H&E; Magnification X160).